

Alma Mater Studiorum Università di Bologna
Archivio istituzionale della ricerca

Local cardinal interpolation by C^2 cubic B2-splines with a tunable shape parameter

This is the final peer-reviewed author's accepted manuscript (postprint) of the following publication:

Published Version:

Romani Lucia (2019). Local cardinal interpolation by C^2 cubic B2-splines with a tunable shape parameter. APPLIED MATHEMATICS LETTERS, 94, 13-20 [10.1016/j.aml.2019.02.017].

Availability:

This version is available at: <https://hdl.handle.net/11585/669032> since: 2021-02-21

Published:

DOI: <http://doi.org/10.1016/j.aml.2019.02.017>

Terms of use:

Some rights reserved. The terms and conditions for the reuse of this version of the manuscript are specified in the publishing policy. For all terms of use and more information see the publisher's website.

This item was downloaded from IRIS Università di Bologna (<https://cris.unibo.it/>).
When citing, please refer to the published version.

(Article begins on next page)

This is the final peer-reviewed accepted manuscript of:

Lucia Romani: Local cardinal interpolation by C2 cubic B2-splines with a tunable shape parameter, Applied Mathematics Letters, Volume 94, 2019, Pages 13-20

The final published version is available online at:

<https://doi.org/10.1016/j.aml.2019.02.017>

Rights / License:

The terms and conditions for the reuse of this version of the manuscript are specified in the publishing policy. For all terms of use and more information see the publisher's website.

This item was downloaded from IRIS Università di Bologna (<https://cris.unibo.it/>)

When citing, please refer to the published version.

Local cardinal interpolation by C^2 cubic B2-splines with a tunable shape parameter

Lucia Romani^{a,*}

^a*Dipartimento di Matematica, Alma Mater Studiorum Università di Bologna, P.zza di Porta San Donato 5, Bologna, Italy*

Abstract

A C^2 cubic local interpolating B2-spline, controllable by a shape parameter, is introduced and its properties analyzed. An algorithm for the automatic selection of the free parameter is developed and tested on several examples. Finally, a two-phase subdivision scheme for its efficient evaluation at dyadic points is presented.

Keywords: Cardinal interpolation; Locality; Splines; Shape parameter; Subdivision

1. Introduction

B2-splines [2, 4–6] are piecewise-polynomial, compactly supported fundamental functions for interpolation, that are made of two polynomial pieces between each pair of interpolation nodes. We assume the interpolation nodes to be placed at $j \in \mathbb{Z}$, and we place the joint between the two polynomial pieces defined on the interval $[j, j+1]$ at the midpoint $j + \frac{1}{2}$. The main result of this manuscript deals with the proposal of a new class of B2-spline basis functions for local cardinal interpolation: they are piecewisely defined on the compact support $[-3, 3]$ by C^2 -joined cubic polynomial pieces whose expressions generalize those in [6] by the introduction of a shape parameter. More precisely, in Section 2 we define the new class of fundamental functions, we show that each member of the class can be written as a linear combination of shifted cubic B-splines on the half integer grid, and that the coefficients of the linear combination depend on a free parameter that can be used to globally modify the shape of the fundamental function. Following the line of reasoning in [7, Prop.1], we prove that the integer shifts of each fundamental function form a Riesz basis and, depending on the value of the free parameter, reproduce either linear or cubic polynomials. Then, in Section 3 we exploit the newly derived fundamental functions for 2D data interpolation, show how the resulting C^2 interpolating curve can be efficiently generated via a two-phase subdivision scheme and develop an algorithm for the automatic selection of the shape parameter.

2. Parameter-dependent C^2 cubic B2-spline basis functions for local cardinal interpolation

We modify the definition of the C^2 cubic B2-spline basis function in [6] by making all of its cubic pieces defined in $[-3, 3]$ depend on a free parameter $0 \leq v < +\infty$, so that its explicit expression becomes

$$\phi_v(t) = \begin{cases} \phi_{v,\ell}(|t|), & \frac{\ell-1}{2} \leq |t| < \frac{\ell}{2}, \ell = 1, \dots, 6 \\ 0, & |t| \geq 3 \end{cases} \quad (2.1)$$

*Corresponding author

Email address: `lucia.romani@unibo.it` (Lucia Romani)

$$\begin{aligned}
& \phi_{v,1}(|t|) = \frac{1}{12}(26 - 11v)|t|^3 + \frac{3}{4}(v - 4)|t|^2 + 1, & 0 \leq |t| < \frac{1}{2}, \\
& \phi_{v,2}(|t|) = \frac{(|t| - \frac{1}{2})}{12} (5(v + 2)|t|^2 - 2(5v + 1)|t| + 2v - 14), & \frac{1}{2} \leq |t| < 1, \\
& \phi_{v,3}(|t|) = \frac{(|t| - \frac{1}{2})}{24} ((9v - 28)|t|^2 + (92 - 18v)|t| + 3v - 76), & 1 \leq |t| < \frac{3}{2}, \\
& \phi_{v,4}(|t|) = -\frac{(|t| - \frac{3}{2})}{24} ((15v - 4)|t|^2 + (16 - 51v)|t| + 39v - 16), & \frac{3}{2} \leq |t| < 2, \\
& \phi_{v,5}(|t|) = \frac{v}{24} (7|t|^3 - 51|t|^2 + 123|t| - 98), & 2 \leq |t| < \frac{5}{2}, \\
& \phi_{v,6}(|t|) = -\frac{v}{24} (|t| - 3)^3, & \frac{5}{2} \leq |t| < 3.
\end{aligned} \tag{2.2}$$

The parameter-dependent cubic polynomial pieces in (2.2) are defined in such a way that, for any value of v , the fundamental function ϕ_v is symmetric with respect to the y -axis (i.e., $\phi_v(t) = \phi_v(-t)$, $t \in \mathbb{R}$), interpolatory (i.e., $\phi_v(j) = \delta_{0,j}$, $j \in \mathbb{Z}$ with $\delta_{0,j}$ the Kronecker delta) and satisfies Propositions 2.1, 2.2, 2.3.

Proposition 2.1. Denoting by $N_4(2t)$ the cubic B-spline supported on $[-1, 1]$ and having knots at $-1, -\frac{1}{2}, 0, \frac{1}{2}, 1$, we can rewrite the fundamental function ϕ_v in (2.1)-(2.2) in terms of the integer shifts of $N_4(2t)$ as

$$\phi_v(t) = \sum_{j=-4}^4 c_{v,j} N_4(2t - j), \tag{2.3}$$

$$\text{with } c_{v,\pm 4} = \frac{v}{32}, \quad c_{v,\pm 3} = -\frac{v}{8}, \quad c_{v,\pm 2} = -\frac{1}{8}, \quad c_{v,\pm 1} = \frac{1}{2} + \frac{v}{8}, \quad c_{v,0} = \frac{5}{4} - \frac{v}{16}. \tag{2.4}$$

Proof: Since $\phi_v(t) = \phi_v(-t)$, $\forall t \in \mathbb{R}$, we can confine the proof to the case $t \geq 0$. If, for each $i = 0, \dots, 8$, we denote the four polynomial pieces of the cubic B-spline having support $[-3 + \frac{i}{2}, -1 + \frac{i}{2}]$ by

$$\begin{aligned}
S_{-3+\frac{i}{2},1}(t) &:= \frac{4}{3}t^3 - 2(i-6)t^2 + (i-6)^2t - \frac{1}{6}(i-6)^3, \\
S_{-3+\frac{i}{2},2}(t) &:= -4t^3 + 2(3i-14)t^2 - (3i-16)(i-4)t + \frac{1}{2}(i-4)^2(i-6) + \frac{2}{3}, \\
S_{-3+\frac{i}{2},3}(t) &:= 4t^3 - 2(3i-10)t^2 + (3i-8)(i-4)t - \frac{1}{2}(i-4)^2(i-2) + \frac{2}{3}, \\
S_{-3+\frac{i}{2},4}(t) &:= -\frac{4}{3}t^3 + 2(i-2)t^2 - (i-2)^2t + \frac{1}{6}(i-2)^3,
\end{aligned}$$

then we can express the six polynomial pieces of ϕ_v defined for $t \geq 0$ as

$$\phi_v(t) = \begin{cases} (\frac{1}{2} + \frac{v}{8})S_{-\frac{3}{2},4}(t) + (\frac{5}{4} - \frac{v}{16})S_{-1,3}(t) + (\frac{1}{2} + \frac{v}{8})S_{-\frac{1}{2},2}(t) - \frac{1}{8}S_{0,1}(t), & 0 \leq t < \frac{1}{2}, \\ (\frac{5}{4} - \frac{v}{16})S_{-1,4}(t) + (\frac{1}{2} + \frac{v}{8})S_{-\frac{1}{2},3}(t) - \frac{1}{8}S_{0,2}(t) - \frac{v}{8}S_{\frac{1}{2},1}(t), & \frac{1}{2} \leq t < 1, \\ (\frac{1}{2} + \frac{v}{8})S_{-\frac{1}{2},4}(t) - \frac{1}{8}S_{0,3}(t) - \frac{v}{8}S_{\frac{1}{2},2}(t) + \frac{v}{32}S_{1,1}(t), & 1 \leq t < \frac{3}{2}, \\ -\frac{1}{8}S_{0,4}(t) - \frac{v}{8}S_{\frac{1}{2},3}(t) + \frac{v}{32}S_{1,2}(t), & \frac{3}{2} \leq t < 2, \\ -\frac{v}{8}S_{\frac{1}{2},4}(t) + \frac{v}{32}S_{1,3}(t), & 2 \leq t < \frac{5}{2}, \\ \frac{v}{32}S_{1,4}(t), & \frac{5}{2} \leq t < 3, \end{cases}$$

so obtaining the claimed result. ■

Proposition 2.2. The family of functions $\{\phi_v(\cdot - n)\}_{n \in \mathbb{Z}}$ forms a Riesz basis for the space $V(\phi_v) = \{s(t) = \sum_{n \in \mathbb{Z}} q_n \phi_v(t - n) : \mathbf{q} = (q_n)_{n \in \mathbb{Z}} \in \ell_2(\mathbb{Z})\}$, and thus the integer shifts of the fundamental function ϕ_v in (2.1)-(2.2) are linearly independent.

Proof: The family of functions $\{\phi_v(\cdot - n)\}_{n \in \mathbb{Z}}$ forms a Riesz basis for the space $V(\phi_v)$ if and only if there exist two constants $A_v > 0$ and $B_v < +\infty$ such that

$$A_v \|\mathbf{q}\|_{\ell_2(\mathbb{Z})} \leq \left\| \sum_{n \in \mathbb{Z}} q_n \phi_v(\cdot - n) \right\|_{L_2(\mathbb{R})} \leq B_v \|\mathbf{q}\|_{\ell_2(\mathbb{Z})} \tag{2.5}$$

for any sequence $\mathbf{q} = (q_n)_{n \in \mathbb{Z}} \in \ell_2(\mathbb{Z})$. Condition (2.5) is equivalent to the Fourier-domain condition

$$A_v^2 \leq \sum_{h \in \mathbb{Z}} \left| \hat{\phi}_v(\omega - 2h\pi) \right|^2 \leq B_v^2, \quad \forall \omega \in \mathbb{R}, \tag{2.6}$$

where $\hat{f}(\omega) := \int_{-\infty}^{+\infty} f(t)e^{-i\omega t}dt$ denotes the Fourier transform of $f(t)$ [8]. Let $\mathbf{c}_v = (c_{v,n})_{n \in \mathbb{Z}}$ be the sequence obtained from the coefficients in (2.4) by considering also $c_{v,n} = 0$ if $|n| \geq 5$. To prove (2.6), we first write the Fourier transform of (2.3) as

$$\hat{\phi}_v(\omega) = \frac{1}{2}G(\omega)\hat{N}_4\left(\frac{\omega}{2}\right) \quad \text{with} \quad G(\omega) := \sum_{n \in \mathbb{Z}} c_{v,n} e^{-i\omega \frac{n}{2}}, \quad (2.7)$$

and then we focus separately on the existence of the lower bound A_v and the upper bound B_v . As we will see, the existence of an upper bound relies on the one for cubic B-splines, while the existence of a lower bound is based on the fact that ϕ_v is interpolatory.

Upper bound. We start by observing that $G(\omega - 2h\pi) = \sum_{n \in \mathbb{Z}} ((-1)^h)^n c_{v,n} e^{-i\omega \frac{n}{2}}$ for all $h \in \mathbb{Z}$. Thus,

$$G(\omega - 2h\pi) = \begin{cases} \sum_{n \in \mathbb{Z}} c_{v,n} e^{-i\omega \frac{n}{2}} =: G_0(\omega), & \text{if } h \text{ even integer,} \\ \sum_{n \in \mathbb{Z}} (-1)^n c_{v,n} e^{-i\omega \frac{n}{2}} =: G_1(\omega), & \text{if } h \text{ odd integer,} \end{cases}$$

and, exploiting (2.7), we can write

$$\sum_{h \in \mathbb{Z}} \left| \hat{\phi}_v(\omega - 2h\pi) \right|^2 = \frac{1}{4} |G_0(\omega)|^2 \sum_{h \in \mathbb{Z}} \left| \hat{N}_4\left(\frac{\omega}{2} - 2h\pi\right) \right|^2 + \frac{1}{4} |G_1(\omega)|^2 \sum_{h \in \mathbb{Z}} \left| \hat{N}_4\left(\frac{\omega}{2} - (2h+1)\pi\right) \right|^2.$$

Taking into account that $|G_l(\omega)| \leq \sum_{n \in \mathbb{Z}} |c_{v,n}| = \|\mathbf{c}_v\|_{\ell_1(\mathbb{Z})}$, for $l = 0, 1$, we obtain the inequality

$$\sum_{h \in \mathbb{Z}} \left| \hat{\phi}_v(\omega - 2h\pi) \right|^2 \leq \frac{1}{4} \|\mathbf{c}_v\|_{\ell_1(\mathbb{Z})}^2 \sum_{h \in \mathbb{Z}} \left| \hat{N}_4\left(\frac{\omega}{2} - h\pi\right) \right|^2.$$

Now let $\mathbf{b} = (b_n)_{n \in \mathbb{Z}}$ with $b_n = (N_4 * N_4^-)(n)$ and $N_4^-(t) = N_4(-t)$. Since

$$(\widehat{N_4 * N_4^-})(\omega) = \hat{N}_4(\omega) \hat{N}_4^-(\omega) = \hat{N}_4(\omega) \hat{N}_4(-\omega) = \hat{N}_4(\omega) \overline{\hat{N}_4(\omega)} = |\hat{N}_4(\omega)|^2,$$

then recalling Poisson's summation formula $\sum_{h \in \mathbb{Z}} \hat{f}\left(\omega - \frac{2h\pi}{T}\right) = T \sum_{n \in \mathbb{Z}} f(nT) e^{-i\omega n T}$ for $\omega \in \mathbb{R}$, $T > 0$, we can write

$$\sum_{h \in \mathbb{Z}} \left| \hat{N}_4\left(\frac{\omega}{2} - h\pi\right) \right|^2 = \sum_{h \in \mathbb{Z}} (\widehat{N_4 * N_4^-})\left(\frac{\omega}{2} - h\pi\right) = 2 \sum_{n \in \mathbb{Z}} b_{2n} e^{-i\omega n} \leq 2 \|\mathbf{b}\|_{\ell_1(\mathbb{Z})} =: B^2.$$

In view of the fact that the function $N_4 * N_4^-$ is continuous and compactly supported, it follows that the sequence \mathbf{b} of its samples is in $\ell_1(\mathbb{Z})$ and then $B^2 < +\infty$. In light of (2.4) also $\|\mathbf{c}_v\|_{\ell_1(\mathbb{Z})}^2 < +\infty$ for any

$0 \leq v < +\infty$. As a consequence, $\sum_{h \in \mathbb{Z}} \left| \hat{\phi}_v(\omega - 2h\pi) \right|^2 \leq \frac{1}{4} \|\mathbf{c}_v\|_{\ell_1(\mathbb{Z})}^2 B^2 =: B_v^2$, and thus the constant $B_v = \frac{1}{2} \|\mathbf{c}_v\|_{\ell_1(\mathbb{Z})} B < +\infty$ acts as an upper bound in (2.6).

Lower bound. Exploiting the fact that ϕ_v is interpolatory, we know that its Fourier transform satisfies [9]

$$\sum_{h \in \mathbb{Z}} \hat{\phi}_v(\omega - 2h\pi) = 1, \quad \forall \omega \in \mathbb{R}. \quad (2.8)$$

In addition, the function $H(\omega) := \sum_{h \in \mathbb{Z}} \left| \hat{\phi}_v(\omega - 2h\pi) \right|^2$ is continuous and periodic since the functions $G_0(\omega)$, $G_1(\omega)$ and $\omega \mapsto \sum_{h \in \mathbb{Z}} \left| \hat{N}_4\left(\frac{\omega}{2} - h\pi\right) \right|^2$ are all continuous and periodic. There follows that $H(\omega)$ reaches its minimum at some $\omega_0 \in [0, 2\pi]$. Thus, we can define the constant $A_v^2 := H(\omega_0)$ which clearly satisfies the inequality $A_v^2 \geq 0$. But, if we assume $A_v = 0$, then we have $\hat{\phi}_v(\omega_0 - 2h\pi) = 0$ for all $h \in \mathbb{Z}$, which contradicts (2.8). Hence it must necessarily be $A_v > 0$. This proves the existence of the lower bound in (2.6). ■

Within the class of parameter-dependent C^2 cubic B2-spline basis functions, we can identify two special members:

- the one having the shortest support (i.e., $[-2, 2]$), which is obtained for $v = 0$ (already studied in [5]);
- the *optimal* one in the sense of Dahmen-Goodman-Micchelli [4], which is the one having approximation order 4 and is obtained for $v = \frac{2}{3}$ (already studied in [4, 6]).

The basis functions ϕ_0 and $\phi_{2/3}$ are illustrated in Figure 1 together with the shifts of the cubic B-spline $N_4(2\cdot)$ involved in their construction.

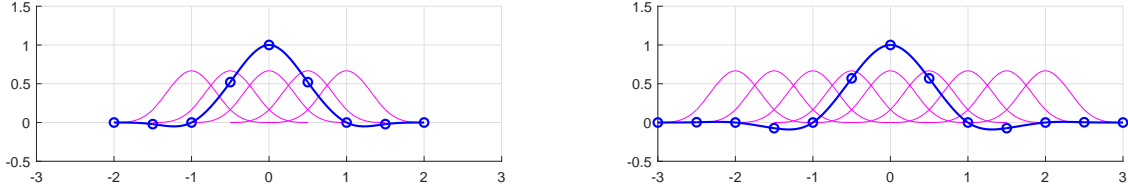


Figure 1: The B2-spline basis functions ϕ_0 (left) and $\phi_{2/3}$ (right) with their cubic polynomial pieces, and the underlined shifts of the cubic B-spline dilated by a factor of 2.

The property of optimality is based on the result proven in the next proposition.

Proposition 2.3. *Let Π^d denote the set or linear space of all polynomials of degree $\leq d$. The integer shifts of the fundamental function ϕ_v in (2.1)-(2.2) can reproduce Π^1 for all $0 \leq v < +\infty$ and Π^3 for $v = \frac{2}{3}$.*

Proof: We start by writing

$$\sum_{i=-2}^3 i^\ell \phi_v(t-i) = \begin{cases} f_L^{[\ell]}(t) & \text{if } t \in [0, \frac{1}{2}), \\ f_R^{[\ell]}(t) & \text{if } t \in [\frac{1}{2}, 1] \end{cases} \quad \text{with} \quad \begin{aligned} f_L^{[\ell]}(t) &= \sum_{i=-2}^0 i^\ell \phi_{v,1-2i}(t-i) + \sum_{i=1}^3 i^\ell \phi_{v,2i}(-t+i), \\ f_R^{[\ell]}(t) &= \sum_{i=-2}^0 i^\ell \phi_{v,2-2i}(t-i) + \sum_{i=1}^3 i^\ell \phi_{v,2i-1}(-t+i). \end{aligned}$$

These expressions, together with (2.2), yield $f_L^{[0]}(t) = f_R^{[0]}(t) = 1$, $f_L^{[1]}(t) = f_R^{[1]}(t) = t$ for all $0 \leq v < +\infty$,

$$\text{and} \quad \begin{aligned} f_L^{[2]}(t) &= -\frac{1}{3}t^2(4(2-3v)t + 9(v-1)), & f_R^{[2]}(t) &= -\frac{1}{3}(4(3v-2)t^3 + 3(5-9v)t^2 + 6(3v-2)t - 3v + 2), \\ f_L^{[3]}(t) &= -\frac{1}{2}t(2(1-3v)t^2 + 3v-2), & f_R^{[3]}(t) &= -\frac{1}{2}(2(9v-7)t^3 + 12(2-3v)t^2 + 7(3v-2)t - 3v + 2). \end{aligned}$$

There follows that $f_L^{[2]}(t) = f_R^{[2]}(t) = t^2 \Leftrightarrow v = \frac{2}{3}$ and $f_L^{[3]}(t) = f_R^{[3]}(t) = t^3 \Leftrightarrow v = \frac{2}{3}$. ■

3. C^2 cubic B2-spline interpolating curves with variable shape parameter

Denoting by $\{\bar{P}_i^0, i \in \mathbb{Z}\}$ the vertices of a given polygon, we can construct the interpolating curve based on the B2-spline fundamental function ϕ_v as

$$s(t) = \sum_{i \in \mathbb{Z}} \bar{P}_i^0 \phi_v(t-i), \quad t \in I \subset \mathbb{R}. \quad (3.1)$$

Due to the special expression of the compactly supported function ϕ_v , we can write $s(t) = \bigcup_{i \in \mathbb{Z}} s_i(t)$, where each curve piece $s_i(t)$, $t \in [0, 1]$, is confined between the pair of consecutive vertices $\bar{P}_i^0, \bar{P}_{i+1}^0$ and reads as

$$s_i(t) = \begin{cases} s_{i,L}(t), & \text{if } t \in [0, \frac{1}{2}), \\ s_{i,R}(t), & \text{if } t \in [\frac{1}{2}, 1] \end{cases} \quad \text{with} \quad \begin{aligned} s_{i,L}(t) &= \sum_{i=-2}^0 \bar{P}_{i+\ell}^0 \phi_{v,1-2i}(t-i) + \sum_{i=1}^3 \bar{P}_{i+\ell}^0 \phi_{v,2i}(-t+i), \\ s_{i,R}(t) &= \sum_{i=-2}^0 \bar{P}_{i+\ell}^0 \phi_{v,2-2i}(t-i) + \sum_{i=1}^3 \bar{P}_{i+\ell}^0 \phi_{v,2i-1}(-t+i). \end{aligned}$$

In particular, $s_{i,L}(0) = \bar{P}_i^0$ and $s_{i,R}(1) = \bar{P}_{i+1}^0$.

3.1. A two-phase subdivision scheme for generating cubic B2-spline interpolants of variable shape

Substituting in (3.1) the expression of ϕ_v given in (2.3), we can rewrite the spline curve s as

$$\begin{aligned} s(t) &= \sum_{i \in \mathbb{Z}} \left(\frac{v}{32} \bar{P}_{i-2}^0 - \frac{1}{8} \bar{P}_{i-1}^0 + \left(\frac{5}{4} - \frac{v}{16} \right) \bar{P}_i^0 - \frac{1}{8} \bar{P}_{i+1}^0 + \frac{v}{32} \bar{P}_{i+2}^0 \right) N_4(2t - 2i) \\ &+ \sum_{i \in \mathbb{Z}} \left(-\frac{v}{8} \bar{P}_{i-1}^0 + \left(\frac{1}{2} + \frac{v}{8} \right) \bar{P}_i^0 + \left(\frac{1}{2} + \frac{v}{8} \right) \bar{P}_{i+1}^0 - \frac{v}{8} \bar{P}_{i+2}^0 \right) N_4(2t - 2i - 1). \end{aligned}$$

Therefore, if we introduce the notation

$$\begin{aligned} P_{2i}^0 &:= \frac{v}{32} \bar{P}_{i-2}^0 - \frac{1}{8} \bar{P}_{i-1}^0 + \left(\frac{5}{4} - \frac{v}{16} \right) \bar{P}_i^0 - \frac{1}{8} \bar{P}_{i+1}^0 + \frac{v}{32} \bar{P}_{i+2}^0, \\ P_{2i+1}^0 &:= -\frac{v}{8} \bar{P}_{i-1}^0 + \left(\frac{1}{2} + \frac{v}{8} \right) \bar{P}_i^0 + \left(\frac{1}{2} + \frac{v}{8} \right) \bar{P}_{i+1}^0 - \frac{v}{8} \bar{P}_{i+2}^0, \end{aligned} \quad (3.2)$$

we can represent the interpolating curve s as a cubic spline curve with control points $\{P_i^0, i \in \mathbb{Z}\}$, i.e., as

$$s(t) = \sum_{i \in \mathbb{Z}} P_i^0 N_4(2t - i).$$

As a consequence, exploiting the refinement equation of cubic B-splines, we can efficiently represent the B2-spline curve interpolating $\{\bar{P}_i^0, i \in \mathbb{Z}\}$ via a subdivision scheme that evaluates it at dyadic points. The subdivision scheme is a *two-phase* subdivision scheme that applies in the first iteration the preprocessing step in (3.2) yielding the new vertex sequence $\{P_i^0, i \in \mathbb{Z}\}$, and in all subsequent iterations the standard refinement rules for cubic splines (see, e.g., [3, Section 2.1]) starting from $\{P_i^0, i \in \mathbb{Z}\}$ (see Figure 3).

3.2. Automatic selection of the global shape parameter v

By varying the free parameter v , the B2-spline basis function ϕ_v is represented by a different graph (see Figure 2 left) and the shape of the interpolating curve in (3.1) changes accordingly (see Figure 2 right). The goal of this section is to propose an automatic selection of the global shape parameter v that, in addition to being driven only by the data to be interpolated, allows one to generate interpolating curves that do not exhibit ugly undulations. Specifically, for any given closed polygon, the algorithm we propose for selecting the shape parameter v in an automatic way, proceeds as described hereafter. Let $\{\bar{P}_i^0 = (x_i, y_i), i = 1, \dots, M\}$ be the distinct vertices of the closed polygon \bar{P}^0 . Then, the control polygon P^0 obtained via (3.2) will consist of $2M$ distinct vertices. We will thus make our selection of v from a set of $2M$ values that is constructed as follows. For all $r = 1, \dots, M$, assume that the coordinate components of each subset of three consecutive vertices $P_j^0 = (x_j^0, y_j^0)$, $j = 2r, 2r+1, 2r+2$ depend on a different parameter v_r , and compute

$$f(v_r) := \left(\langle P_{2r+1}^0 - P_{2r}^0, P_{2r+2}^0 - P_{2r+1}^0 \rangle \right)^2 - \|P_{2r+1}^0 - P_{2r}^0\|_2^2 \|P_{2r+2}^0 - P_{2r+1}^0\|_2^2. \quad (3.3)$$

The function in (3.3) has the explicit expression $f(v_r) = -2^{-20} (a v_r^2 + 4b v_r + 16c)^2$ with

$$\begin{aligned} a &:= (5x_{r-1} - 4x_r - 6x_{r+1} + 4x_{r+2} + x_{r+3})y_{r-2} + (-5x_{r-2} + 14x_r - 4x_{r+1} - 9x_{r+2} + 4x_{r+3})y_{r-1} \\ &+ (4x_{r-2} - 14x_{r-1} + 20x_{r+1} - 4x_{r+2} - 6x_{r+3})y_r + (6x_{r-2} + 4x_{r-1} - 20x_r + 14x_{r+2} - 4x_{r+3})y_{r+1} \\ &+ (-4x_{r-2} + 9x_{r-1} + 4x_r - 14x_{r+1} + 5x_{r+3})y_{r+2} + (-x_{r-2} - 4x_{r-1} + 6x_r + 4x_{r+1} - 5x_{r+2})y_{r+3}, \\ b &:= (-5x_r + 6x_{r+1} - x_{r+2})y_{r-2} + (-46x_r + 55x_{r+1} - 8x_{r+2} - x_{r+3})y_{r-1} \\ &+ (5x_{r-2} + 46x_{r-1} - 112x_{r+1} + 55x_{r+2} + 6x_{r+3})y_r + (-6x_{r-2} - 55x_{r-1} + 112x_r - 46x_{r+2} - 5x_{r+3})y_{r+1} \\ &+ (x_{r-2} + 8x_{r-1} - 55x_r + 46x_{r+1})y_{r+2} + (x_{r-1} - 6x_r + 5x_{r+1})y_{r+3}, \\ c &:= (5x_r - 6x_{r+1} + x_{r+2})y_{r-1} + (-5x_{r-1} + 11x_{r+1} - 6x_{r+2})y_r + (6x_{r-1} - 11x_r + 5x_{r+2})y_{r+1} \\ &+ (-x_{r-1} + 6x_r - 5x_{r+1})y_{r+2}. \end{aligned}$$

If $b^2 - 4ac \geq 0$, then $v_r = 2 \frac{-b \pm \sqrt{b^2 - 4ac}}{a}$ are real roots of f , which can be conveniently distinguished by introducing the notation $v_{r,1} := 2 \frac{-b + \sqrt{b^2 - 4ac}}{a}$ and $v_{r,2} := 2 \frac{-b - \sqrt{b^2 - 4ac}}{a}$. Note that, in light of (3.3), if v_r takes one of these values, then the consecutive control points $P_{2r}^0, P_{2r+1}^0, P_{2r+2}^0$ are aligned. Conversely, if $b^2 - 4ac < 0$, we assume that two real values are assigned to $v_{r,1}$ and $v_{r,2}$ by the user. For instance, the special values $\frac{2}{3}$ and 0, respectively providing the B2-spline basis function with the highest approximation order and the smallest support could be selected, as well as the mean value of the two. Once all the $2M$ values $\{v_{r,1}, v_{r,2}\}_{r=1,\dots,M}$ are known, we select the global shape parameter v in a different way depending if \bar{P}^0 is a globally convex polygon or a non-convex polygon (for the meaning of these terms we refer the reader to [1]). Specifically, in the case of globally convex data we simply select

$$v = \max_{r \in \{1,\dots,M\}} \{v_{r,2} : 0 \leq v_{r,2} < 1\}.$$

Differently, in the case of non-convex data, let $\bar{P}_m^0 = (x_m, y_m)$ be the vertex that satisfies $\angle(\bar{P}_{m-1}^0, \bar{P}_m^0, \bar{P}_{m+1}^0) = \max_{i=1,\dots,M} \angle(\bar{P}_{i-1}^0, \bar{P}_i^0, \bar{P}_{i+1}^0)$ where $\bar{P}_0^0 := \bar{P}_M^0$ and $\bar{P}_{M+1}^0 := \bar{P}_1^0$. Then, we define

$$r^* = \begin{cases} m, & \text{if } \|\bar{P}_{m+1}^0 - \bar{P}_m^0\|_2 \leq \|\bar{P}_m^0 - \bar{P}_{m-1}^0\|_2 \\ m-1, & \text{otherwise} \end{cases} \quad \text{and} \quad v = \begin{cases} \max\{v_{r^*,1}, v_{r^*,2}\}, & \text{if } v_{r^*,1} v_{r^*,2} \leq 0 \\ \min\{v_{r^*,1}, v_{r^*,2}\}, & \text{if } v_{r^*,1} v_{r^*,2} > 0. \end{cases}$$

Examples of closed curves interpolating non-convex data and globally convex data, for which the shape parameter v is computed via the previously described algorithm, are displayed in Figures 3 and 4, respectively. Although we cannot claim that the interpolants obtained from the computed values of v always preserve the local/global convexity of the data, our numerical experiments have shown that they do not exhibit ugly undulations and, in many cases, they behave also better than the C^2 cubic B2-spline interpolants proposed in [4–6] (see Figure 5).

References

- [1] G. Albrecht, L. Romani, Convexity preserving interpolatory subdivision with conic precision, *Appl. Math. Comput.* 219, 4049–4066 (2012)
- [2] M. Antonelli, C.V. Beccari, G. Casciola, A general framework for the construction of piecewise-polynomial local interpolants of minimum degree, *Adv. Comput. Math.* 40, 945–976 (2014)
- [3] C. Conti, M. Cotronei, L. Romani, Beyond B-splines: exponential pseudo-splines and subdivision schemes reproducing exponential polynomials, *Dolomites Research Notes on Approximation* 10, 31–42 (2017)
- [4] W. Dahmen, T. Goodman, C.A. Micchelli, Compactly supported fundamental functions for spline interpolation, *Numer. Math.* 52, 639–664 (1988)
- [5] M. Kuroda, S. Furukawa, F. Kimura, Controllable locality in C^2 interpolating curves by B2-splines/S-splines, *Computer Graphics Forum* 13(1), 49–55 (1994)
- [6] D.X. Qi, A class of local explicit many-knot spline interpolation schemes, *Univ. of Wisconsin, MRC TSR #2238* (1981)
- [7] D. Schmitter, J. Fageot, A. Badoual, P. Garcia-Amorena, M. Unser, Compactly-supported smooth interpolators for shape modeling with varying resolution, *Graphical Models* 94, 52–64 (2017)
- [8] M. Unser, T. Blu, Cardinal exponential splines: part I - theory and filtering algorithms, *IEEE Transactions on Signal Processing* 53(4), 1425–1438 (2005)
- [9] M. Unser, P. Thévenaz, L. Yaroslavsky, Convolution-based interpolation for fast, high-quality rotation of images, *IEEE Transactions on Image Processing* 4(10), 1371–1381 (1995)

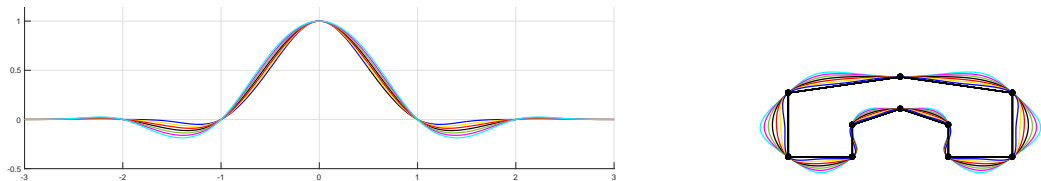


Figure 2: Comparison of B2-spline basis functions (left) and corresponding data interpolation (right) for the following values of v (from inner to outer): 0 (blue), $\frac{1}{3}$ (yellow), $\frac{2}{3}$ (red), 1 (black), $\frac{4}{3}$ (green), $\frac{5}{3}$ (magenta), 2 (cyan).

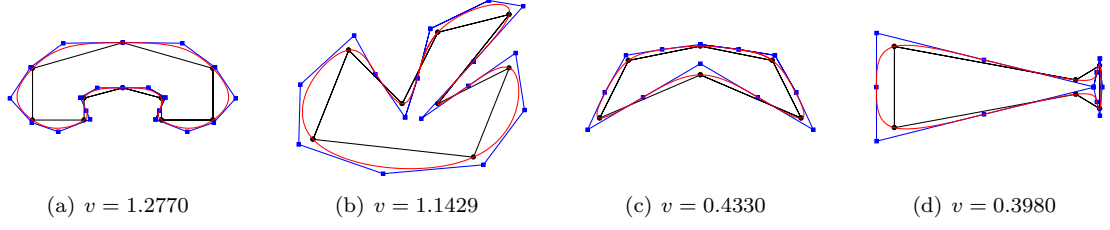


Figure 3: Interpolation data $\{\bar{P}_i^0, i = 1, \dots, M\}$ (black bullets), initial vertices of the subdivision process $\{P_i^0, i = 1, \dots, 2M\}$ (blue squares), interpolating curve generated via cubic spline refinement of $\{P_i^0, i = 1, \dots, 2M\}$ with automatically computed parameter v (red).

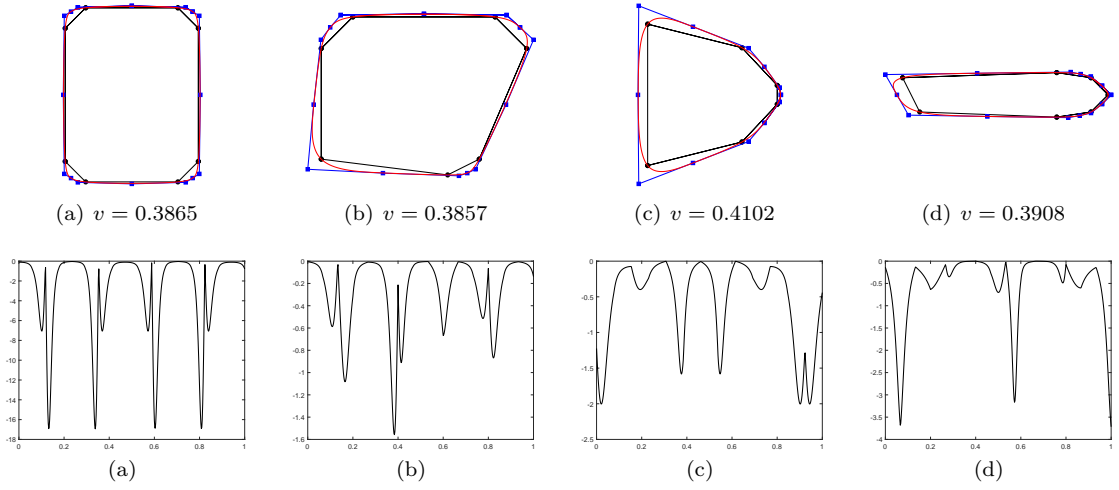


Figure 4: First row: globally convex interpolation data $\{\bar{P}_i^0, i = 1, \dots, M\}$ (black bullets), initial vertices of the subdivision process $\{P_i^0, i = 1, \dots, 2M\}$ (blue squares), convex interpolating curve generated via cubic spline refinement of $\{P_i^0, i = 1, \dots, 2M\}$ with automatically computed parameter v (red). Second row: corresponding curvature plot of constant sign.

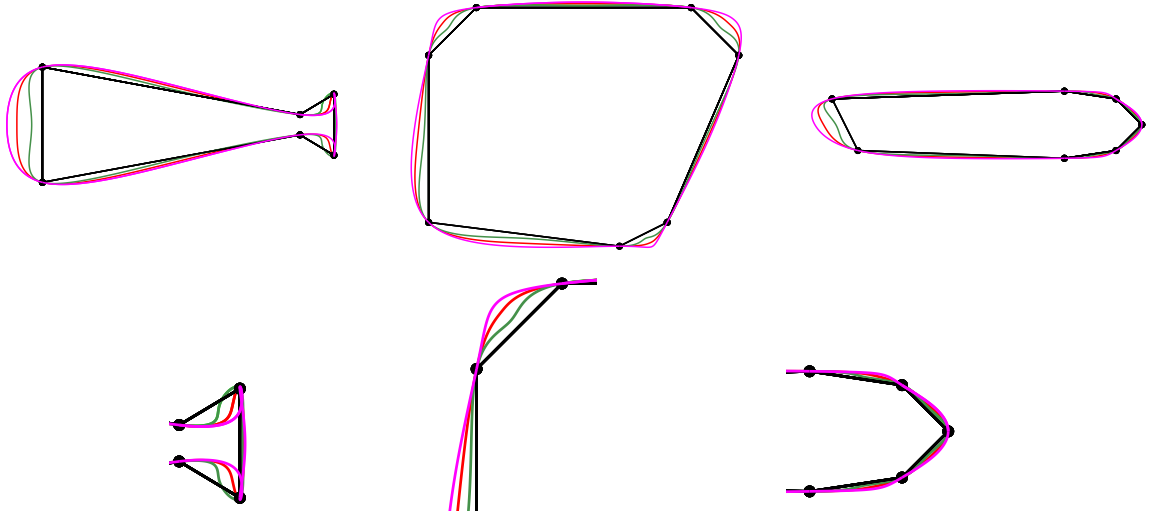


Figure 5: First row: Interpolating curves obtained from the data in Figure 3(d) and Figure 4(b,d) when using $v = 0$ (green), $v = \frac{2}{3}$ (magenta) and v provided by the automatic algorithm (red). (For interpretation of the references to color and for a better comparison between the curves, the reader is referred to the electronic version of this paper.) Second row: enlargement of a detail from each figure in the first row.